A GLUE-based assessment of WaTEM/SEDEM for simulating soil erosion, transport, and deposition in soil conservation optimised agricultural watersheds

Kay D. Seufferheld[1], Pedro V. G. Batista[1], Hadi Shokati[2], Thomas Scholten[2], Peter Fiener[1]

[1]Institute of Geography, Water and Soil Resources Research, University of Augsburg, Augsburg, 86159, Germany.
[2]Department of Geosciences, Soil Science and Geomorphology, University of Tübingen, 72074, Tübingen, Germany.

Correspondence to: Peter Fiener (peter.fiener@geo.uni-augsburg.de, Alter Postweg 118, 56159 Augsburg, Germany)

Abstract. Soil erosion models are ~~essential~~ important tools for soil conservation planning. Although these models are generally well-tested against plot and field data for in-field soil management, challenges arise when scaling up to the landscape level, where sediment trapping along landscape features becomes increasingly critical. At this scale, a separate analysis of model performance for~~in~~ representing erosion, sediment transport, and deposition processes is both challenging and often lacking. Here~~In this study~~, we assessed the capacity of the spatially distributed erosion and sediment transport model WaTEM/SEDEM to simulate sediment yields in six highly instrumented micro-scale watersheds ranging from 0.8 to 7.8 ha, monitored over eight years from 1994 to 2001, in Southern Germany. The watersheds were composed~~comprised~~ of two groups: four field-dominated watersheds characterised by arable land with minimal landscape structures, and two structure-dominated watersheds featuring a combination of arable land and linear landscape structures (mainly grassed waterways along thalwegs) that minimise sediment connectivity. Arable fields in both watershed groups were managed for soil conservation, including no-till and optimised crop rotations. ~~This setup enabled a separate analysis of model performance for both watershed groups.~~ A Generalised Likelihood Uncertainty Estimation (GLUE) framework was employed to account for measurement and model uncertainties across multiple spatiotemporal scales. Our results show that while WaTEM/SEDEM ~~generally~~ captured the magnitude of the very low measured sediment yields in the monitored watersheds, the model did not meet our pre-defined limits of acceptability when operating on annual time steps. ~~However, the WaTEM/SEDEM´s~~Model performance improved substantially when ~~model realisations~~outputs were averaged over the eight-year monitoring period~~aggregated across the eight-year monitoring period and over the two watershed groups~~, with mean absolute errors of 0.~~11~~ 14 t ha^{-1} yr^{-1} for field-dominated and 0.~~18~~ 29 t ha^{-1} yr^{-1} for structure-dominated watersheds. Our findings demonstrate that ~~the model~~WaTEM/SEDEM can represent the influence of soil conservation ~~measures~~ practices on reducing soil erosion and sediment ~~delivery~~ yield in our study area. However, the model is fit~~but performs better~~ for long-term conservation planning at larger spatial scales ~~than~~and not for precise annual predictions for~~in~~ individual micro-scale watersheds with specific conservation practices even if high-resolution, high-quality input data are available for parameterisation.

1. Introduction

Soil erosion by water is a major threat to global soil health and associated ecosystem functions and services, endangering agricultural sustainability and food security {Rickson, 2015 #108;Montanarella, 2016 #109;Quinton, 2024 #58}. Although the problem of accelerated soil erosion has been known for a long time and a wide variety of soil conservation practices have been tested and implemented locally for many decades, adoption remains limited due to economic constraints, lack of technical knowledge, and insufficient policy support {Quinton, 2024 #58;Aghabeygi, 2024 #171}. This is particularly problematic in regions where ~~the intensification of~~ agricultur~~al~~e intensification {e.g. field consolidation, soil compaction ~~–~~\Brus, 2018 #144;Keller, 2019 #173;Foucher, 2014 #182;Wang, 2022 #183}~~, exemplified by the historical increase in the size and weight of agricultural machinery that has led to increased soil compaction levels {Brus, 2018 #144;Keller, 2019 #173},~~ and the increase in frequency and intensity of extreme precipitation events due to climate change {Auerswald, 2024 #4;Hosseinzadehtalaei, 2020 #174;Myhre, 2019 #175} ~~is likely~~are exacerbating the erosion ~~risk~~hazards.

Overall, effective soil conservation relies on two complementary strategies: (i) in-field soil conservation and (ii) sediment transport control structures along the flow pathways. In-field practices focus on increasing soil surface cover by vegetation to prevent soil detachment by raindrop impact and overland flow. Such practices include optimised crop rotations, using cover crops, and soil residue management {Andersson, 2014 #145}. Sediment transport control practices consist of structures installed along the runoff pathway to increase infiltration, sediment trapping, and hence minimise sediment connectivity~~Effective soil conservation relies on two complementary strategies: (i) In-field control measures that increase soil surface cover by vegetation and hence prevent soil detachment by raindrop impact and sheet flow. Such measures include optimised crop rotations, using cover crops, and soil residue management {Andersson, 2014 #145}. (ii) Off-site sediment transport control structures along the runoff pathway that increase infiltration and foster sediment trapping and minimise sediment connectivity.~~ Typical structures are vegetative filter strips {Gumiere, 2011 #146}, grassed waterways {Fiener, 2003 #124}, retention ponds {Fiener, 2005 #155}, or ~~a~~ generally optimised layout of fields along slopes {Van Oost, 2000 #117}.

Soil erosion models are potentially valuable tools for identifying erosion-prone areas and developing what-if scenarios, allowing stakeholders to assess different configurations of on- and off-site soil conservation practices. This enables the identification of optimal intervention strategies before implementation.~~Soil erosion models are potentially valuable tools for identifying high erosion risk areas and evaluating intervention needs, enabling stakeholders to effectively implement soil conservation strategies.~~ Diverse models have been developed and applied for this purpose, ranging from empirical or~~and~~ conceptual to process-oriented~~ model types~~ {e.g. \Eekhout, 2018 #59;Smith, 2018 #61;Nearing, 2013 #165;Dymond, 2010 #166;Hessel, 2008 #168}. As indicated by erosion modelling reviews {Batista, 2019 #120;~~}{~~Borrelli, 2021 #184}, the most widely used erosion model is still the empirical Universal Soil Loss Equation {USLE; \Wischmeier, 1978 #17} and its revisions and regional adaptations, such as the revised USLE {RUSLE; \Renard, 1997 #7} and the German ABAG {Allgemeine

Bodenabtragsgleichung, German for Universal Soil Loss Equation; \DIN-Normenausschuss, 2022 #2;{Schwertmann, 1987 #27}} The most widely used model for soil conservation planning is the Universal Soil Loss Equation (USLE) {Wischmeier, 1978 #17} and its revisions and regional adaptations, like the revised USLE (RUSLE) {Renard, 1997 #7} and the German ABAG {Allgemeine Bodenabtragsgleichung`, German for Universal Soil Loss Equation`; \DIN-Normenausschuss, 2022 #28;Schwertmann, 1987 #27}.

While these USLE-type models have been adapted to calculate spatially distributed erosion rates, they are limited to calculating potential soil loss without considering sediment transport processes and downslope deposition. To overcome this limitation, the Water and Tillage Erosion Model and the Sediment Delivery Model (WaTEM/SEDEM) {Van Oost, 2000 #117;Van Rompaey, 2001 #10;Verstraeten, 2002 #119} was developed. WaTEM/SEDEM combines the USLE-technology RUSLE {Renard, 1997 #7} with spatially distributed sediment transport and deposition modelling. The performance of the model has been tested using sediment trapping in reservoirs {e.g. \Hlavčová, 2018 #150}, sediment delivery yield in small rivers of mesoscale catchments {e.g. \Batista, 2022 #96;Rehm, 2024 #152}, andor long-term erosion and deposition patterns derived from radionuclides {e.g. \Van Oost, 2000 #117;Wilken, 2020 #141}. However, to the best of our knowledge, the suitability of WaTEM/SEDEM for representing soil erosion, transport, and deposition processes within soil conservation settings (e.g. no-till, cover crop, optimised crop rotations) combined with sediment transport control structures to reduce sediment connectivity (e.g. grassed water ways, retention ponds), has not been thoroughly tested against measured data{Van Oost, 2000 #117}{Van Rompaey, 2001 #10}. However, to the best of our knowledge, the suitability of WaTEM/SEDEM for representing soil erosion, transport, and deposition processes within soil conservation settings combined with measures to reduce sediment connectivity, which can minimize sediment redistribution, has not been thoroughly tested.

Testing the ability of spatially distributed erosion models to simulate the combined effects of in-field soil conservation and landscape features trapping sediments is inherently challenging. Observational data for model calibration and validation are typically restricted to measurements of sediment yields at the outlet of a system {Batista, 2019 #120}, which typically consist of small erosion plots, meso-scale watersheds, or large-scale catchments. Such outlet-based measurements do not allow for testing a model's representation of internal erosion and deposition patterns, as they provide little information on the spatial distribution of sediment sources and sinks within the landscape.

One difficulty is that most plot-scale data do not account for landscape features, as they are typically not included in plots. Conversely, watershed outlet data may integrate the effects of both in-field soil conservation and sediment transport control structures into one lumped measurement, which makes it difficult to disentangle their individual contributions to (dis)connecting the sediment cascade. Long-term monitoring data from micro-scale watersheds (1-10 ha) offer the opportunity to evaluate in-field soil conservation practices separately from sediment transport control structures implemented at field to the landscape scale {Choudhury, 2022 #69;Fiener, 2018 #54}. However, such datasets are rare {Fiener, 2019 #130}, and erosion and sediment delivery models have hardly been tested under these conditions.

Regardless of the spatial scale in which erosion is monitored, it is important to note that perfect observational data do not exist. All measurements include errors stemming from instrumental precision, temporary malfunctioning, and data handling and processing. These uncertainties have important implications for evaluating erosion models, which cannot be expected to be better than the observational data used for model conditioning and testing {Beven, 2022 #128;Beven, 2019 #160}. One approach for evaluating (uncertain) environmental models is the Generalized Likelihood Uncertainty Estimation (GLUE) framework {Beven, 1992 #129}. GLUE acknowledges that it is not possible to identify a single calibrated parameter set as "correct". Rather, all parameter combinations that produce results within given limits-of-acceptability cannot be rejected {Beven, 2022 #128}. Contrarily, if not a single model realisation encompasses the uncertainty bounds of the observational data, non-behavioural models or model structures can be rejected, which might lead to improvements in terms of understanding and modelling.

Here we employ a rejectionist limits-of-acceptability approach within the GLUE framework to test the widely used WaTEM/SEDEM model for representing soil erosion, transport, and deposition in soil conservation optimised agricultural watersheds, i.e. featuring a combination of in-field practices and sediment transport control structures. Specifically, we aimed to: (i) identify limits of acceptability of model error derived from measurement uncertainty in order to reject non-behavioural model realisations; (ii) develop a two-stage model conditioning process to test the fitness for purpose of WaTEM/SEDEM for representing the effects of both in-field conservation practices and sediment control structures on erosion, transport, and deposition; and (iii) test WaTEM/SEDEM under different levels of temporal (annual vs. eight-year means) and spatial aggregations (individual vs. grouped watersheds). We accomplish these objectives using a comprehensive, long-term monitoring dataset from Southern Germany, which provides high resolution model inputs (e.g. precipitation, crop-specific daily soil cover, etc.), as well as continuous surface runoff and sediment flux data for six micro-scale watersheds under optimised soil conservation and reduced sediment transport {Auerswald, 2001 #154;Auerswald, 2019 #176;Fiener, 2019 #130}.~~This exacerbates the equifinality problem {Beven, 2006 #125}, and models may achieve accurate outputs while incorrectly representing the spatial patterns of erosion and deposition processes within watersheds.~~

~~Micro-scale watersheds (1-10 ha) are ideal for evaluating soil conservation measures typically implemented from the field to the landscape level {Choudhury, 2022 #69;Fiener, 2018 #54}. This is because soil erosion and sediment connectivity processes that are distinguishable at the micro-scale watershed are not represented in small plots or get diluted in large catchment sediment yield observations. Moreover, important input data for erosion modelling, e.g. rainfall, soil management, and land cover, can be monitored and measured with higher detail at the micro-scale, compared to larger areas {Fiener, 2019 #130}. Nevertheless, there is limited research on modelling the combined effects of in-field soil conservation and landscape structures on soil redistribution and sediment delivery at this scale.~~

~~Notwithstanding the spatial extent of (long-term) soil erosion monitoring, measurement uncertainties arise from instrumental precision and temporal instrument malfunctioning, data handling and processing. The uncertainties in observational data have important implications for erosion modelling, as models cannot be expected to be better than the observational data {Beven, 2022 #128;Beven, 2019 #160}.~~

~~The Generalized Likelihood Uncertainty Estimation (GLUE) framework {Beven, 1992 #129} allows for testing environmental models while accounting for the uncertainty in both models and the observational data. In light of inherent measurement uncertainties, GLUE acknowledges that it is not possible to identify a single parameter set as "correct". Rather, all parameter combinations that produce results within the observational uncertainty cannot be rejected. Within the GLUE framework, limits of acceptability are defined to identify which model runs fall within the uncertainty bounds of the measurements {Beven, 2022 #128}. These behavioural models are retained, while non-behavioural models are rejected. This limits-of-acceptability GLUE approach thus provides a systematic methodology to evaluate model performance with uncertain testing data.~~

~~In this study we employ this limit-of-acceptability approach based on the GLUE framework, focusing on three main objectives: (i) testing WaTEM/SEDEM's capability to simulate sediment yields in micro-scale watersheds either characterised by in-field soil conservation or by in-field soil conservation plus linear landscape features designed to trap sediments, (ii) analysing the behaviour of model parameters that control erosion and sediment transport processes, and (iii) assessing the model's performance across different spatiotemporal resolutions through data aggregation. We accomplish these objectives using a comprehensive dataset from a long-term, farm-scale monitoring in Southern Germany, which provides continuous precipitation, surface runoff and sediment flux data from six micro-scale watersheds under optimised soil conservation {Auerswald, 2001 #154;Auerswald, 2019 #176}{Fiener, 2019 #130}.~~

2. Material and methods

2.1 Test site

The test site is part of an experimental farm located in Scheyern, S~~s~~outhern Germany (48°29'45.1"N, 11°26'23.6"E; about 470 m above sea level). It is part of Bavaria's tertiary hill region, an important and productive agricultural landscape in Central Europe. The rolling topography is characterised by predominantly east-facing slopes ranging from 0.4° to 11.5° {Wilken, 2019 #24}. Climate conditions include a mean annual temperature of 8.4 °C and mean annual precipitation of 834 mm (1994-2001), with the highest precipitation occurring between May and July {Fiener, 2019 #130}. Management practices at the farm follow a comprehensive soil conservation philosophy based on two main principles: (i) keeping arable soils covered as long as possible and (ii) reducing hydrological and sedimentological connectivity as far as possible {Fiener, 2019 #130}. Within the watersheds, soils consist predominantly of loamy or silty loamy Cambisols {World Reference Base for Soil Resources (WRB)`, \Schad, 2022 #177}.

The research area comprises six micro-scale watersheds (W01-W06) with a total area of 24 ha and four agricultural fields (F15-F18, Fig. 1). The six watersheds exhibit different landscape connectivity characteristics: W01–W04 (0.8 to 4.2 ha) are classified as field-dominated systems. Despite the presence of retention ponds at the outlets of W01 and W02, these watersheds have no internal linear landscape structures, resulting in sediment

flux pathways governed primarily by topography and the management of the arable fields. In contrast, W05 and W06 are classified as structure-dominated systems due to the presence of a grassed waterway along the thalweg. ~~W01-W04 (0.8 to 4.2 ha) are classified in this study as field-dominated systems due to their structure, with most of their area covered by agricultural fields and minimal landscape structures along sediment flux pathways. In contrast, W05 and W06 are classified as structure-dominated systems due to their configuration, featuring more complex landscapes. The~~ Watershed W06 (5.7 ha) constitutes the upper part of the larger watershed W05 (7.8 ha) (Fiener et al., 2019a).

Three key conservation practices were implemented to minimise hydrological and sedimentological connectivity: (i) an optimised field layout with reduced field sizes adapted to the steep slopes, (ii) retention ponds at watershed outlets, and (iii) a grassed waterway along the main thalweg of W05 and W06 (Fiener et al, 2019a).~~Three key conservation measures were implemented to minimise hydrological and sedimentological connectivity: (i) optimised field layout with fields arranged parallel to contour lines, (ii) retention ponds at field borders, and (iii) a grassed waterway along the main thalweg of W05 and W06~~. The retention ponds were located at the outlets of watersheds W01, W02, W05, and W06 (Fig. 1). Sediment trapping efficiency measurements were conducted for these ponds, revealing an average of 70 ± 14 % {Fiener, 2005 #155}. Additionally, continuous monitoring systems were installed at the outlet of each micro-scale watershed to measure runoff and sediment ~~delivery~~yield. The distinction between field-dominated and structure-dominated watersheds will be used consistently throughout this study.

All fields within the watersheds (F15 to F18 in Fig. 1) were managed using no-till practices with a crop rotation of winter wheat (*Triticum aestivum* L.), maize (*Zea mays* L.), winter wheat, and potatoes (*Solanum tuberosum* L.). This rotation was staggered across the fields, meaning that while the sequence was identical, the specific crop grown each year varied between fields. ~~All fields within the watersheds were managed using no-till practices with a crop rotation of winter wheat, maize, winter wheat, potatoes, whereas the rotation was shifted between the fields (F15-F18, Fig. 1).~~ After winter wheat, mustard was sown as a cover crop. In the case of potatoes, the mustard was sown into the potato dams built in autumn, while direct seeding into the frost-killed~~down-frozen~~ mustard was performed in the following year.

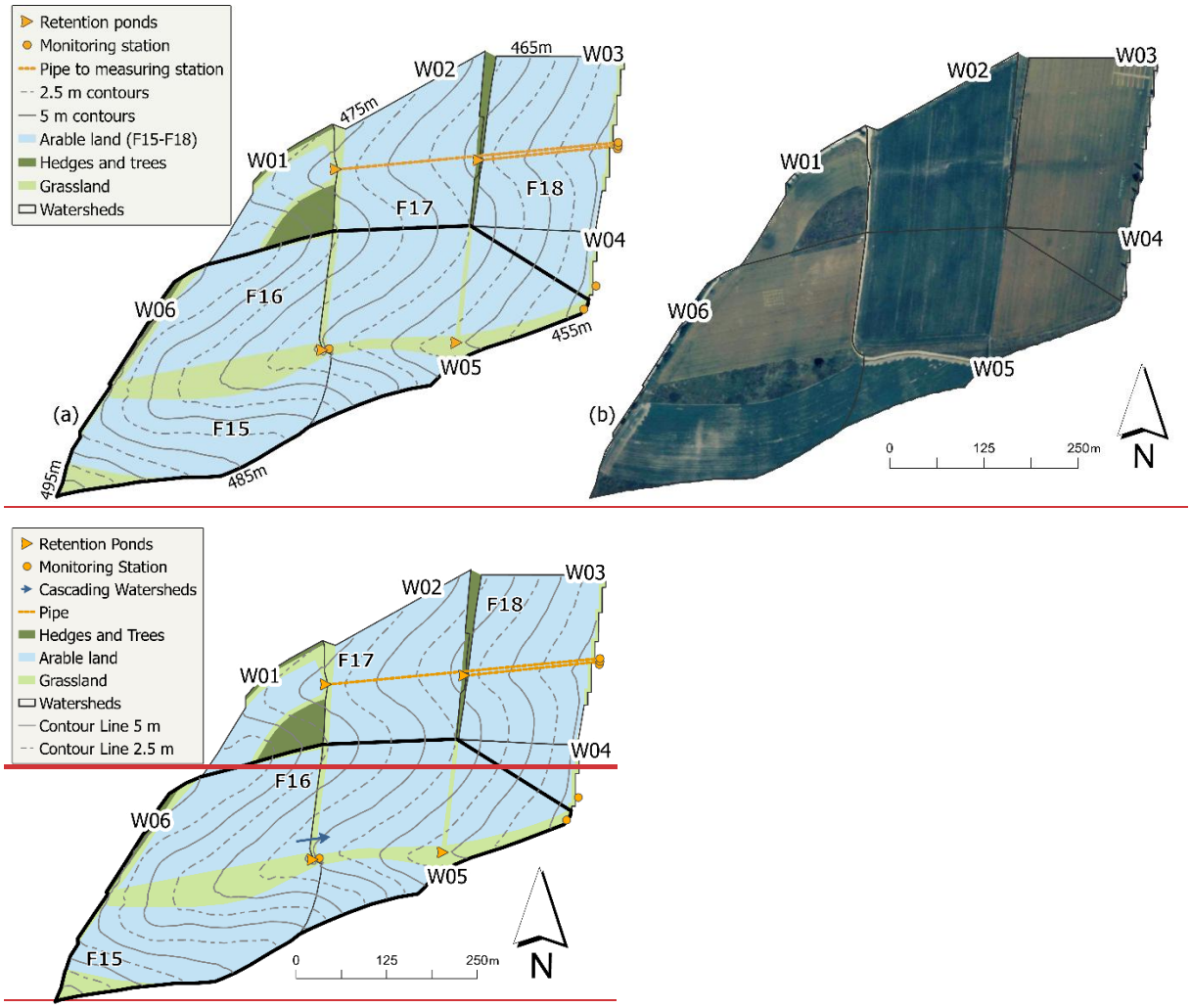

Figure 1: (a) Schematic land use and topography of the experimental farm in Scheyern, Bavaria, with flow direction from west to east. W01-W06 are abbreviations for six watersheds; F15-F18 are the fields located in these watersheds. Note: Watershed W05 (thick line) includes the upslope watershed W06, as W06 is cascading into W05. (b) Aerial photograph of the study area shows the land use patterns and field boundaries on the Scheyern farm in 2002.

2.2 Erosion monitoring data

The study utilised a unique erosion monitoring dataset acquired between 1994 and 2001. This comprehensive dataset, as well as metadata, are provided by {Fiener, 2019 #130@@author-year}. All spatial data were resampled to a consistent 5 m by 5 m grid resolution, matching the digital elevation model (DEM) provided in the dataset {Wilken, 2019 #24}. The temporally dynamic input data included daily soil cover measurements and high-resolution precipitation data recorded at 1-minute intervals from up to 11 monitoring sites {Wilken, 2019 #26}. Additional details regarding these input parameters are provided in section 2.4 below.

For model testing, we used continuous sediment ~~delivery~~ yield data from the six micro-scale watersheds (W01-W06) between 1994 and 2001 (Fig. 1). Runoff and suspended-sediment loads were monitored with a measuring system based on a Coshocton-type wheel sampler {precision ± 10%`; \Carter, 1967 #73;Fiener, 2003 #124}. The device continuously diverted an aliquot of approximately 0.5 % from the total flow that left the watersheds through underground-tile outlets with a diameter of 15.6 cm and 29 cm (Fig. 1) into storage tanks (1.0 – 3.5 m^3).

Runoff volumes were measured after each event. Sediment yield was calculated from runoff volumes and sediment concentrations derived from homogenised tank samples dried at 105°C. At lower rates (< 0.5 L s^{-1}) the system slightly over-estimated runoff, but these small events contributed negligibly to the cumulative water and sediment budgets. Under sampling during very high flows was avoided by (i) employing large wheels (Ø 61 cm) and (ii) the flow-dampening effect of the retention ponds situated immediately upstream of each outlet {Fiener, 2003 #124}.

2.3 Soil erosion modelling

The WaTEM/ SEDEM version used in this study consists of two main components: (i) WaTEM, which implements a spatially distributed German adaption of the USLE {Schwertmann, 1987 #27;DIN-Normenausschuss, 2022 #2}~~{NAW, 2022 #132}~~, and (ii) SEDEM, which incorporates a transport capacity (*TC*) equation (Eq. 43) and a routing algorithm for sediment re-distribution based on the~~a~~ DEM {Verstraeten, 2002 #119;Van Rompaey, 2001 #10;Van Oost, 2000 #117}. To implement WaTEM/ SEDEM within the GLUE-framework, the original Delphi code-based model was translated to Python 3.12 and was run in PyCharm 2024.1 (Community Edition), which substantially improved computational speed through parallel processing and allowed for easier data handling. To ensure reproducibility and accuracy, we compared the Python implementation against the original Delphi codebase at each individual step of the translation process, verifying that it produced identical outputs for these test cases. Although the Python implementation includes tillage erosion and stream initiation calculations, ~~this component~~these components were~~as~~ not utilised in the present study.

The model was applied for the period from April to October of each year from 1994 to 2001, excluding periods potentially affected by snowmelt erosion and prolonged surface runoff from return flow {Fiener, 2019 #130}. While ~~these months~~the colder months contributed 10.7 % of the total measured sediment ~~delivery~~ yield {Fiener, 2019 #99}, our analysis focused on the dominant water erosion period during heavy rainfall months. Each micro-scale watershed was separately modelled.

2.4 Potential ~~e~~E~~E~~rosion

In contrast to the original WaTEM/ SEDEM {Verstraeten, 2002 #119;Van Rompaey, 2001 #10;Van Oost, 2000 #117}, in which the USLE factors are derived according to the RUSLE approach {Renard, 1997 #7}, we calculated the USLE factors as calculated according to their German adaptation (Eq. 1). This approach is specifically adapted to the soils and climatic conditions of Central Europe and represents the standard methodology for the study region {Schwertmann, 1987 #27;DIN-Normenausschuss, 2022 #28}.~~:~~

$$A = R * K * LS * C * P, \quad (1)$$

Where A is the potential erosion (t ha^{-1} yr^{-1}), R the rainfall erosivity factor ~~in~~ (N h^{-1} yr^{-1}), K the soil erodibility factor (t ha^{-1} h N^{-1}), LS the slope length and steepness factor (dimensionless), C the cover management factor (dimensionless), and P the agricultural practices factor (dimensionless).

The high-resolution rainfall data from eleven (1994–1997) and two (1998–2001) precipitation monitoring stations located in the research area were used to calculate the rain erosivity factor (R-factor) {Wilken, 2019 #26}.

~~According to~~Following the German adaptation of the USLE, rainfall events were considered erosive if they met at least one of two criteria: (i) total rainfall amount ≥ 10 mm {in contrast to the 12.7 mm threshold of the standard USLE, \Wischmeier, 1978 #17} or (ii) maximum 30-minute intensity ≥ 10 mm h^{-1}. Individual events were separated by at least 6 hours without rainfall {Schwertmann, 1987 #27;DIN-Normenausschuss, 2022 #28}. The calculated rainfall erosivities per monitoring station were interpolated to 5 m by 5 m resolution maps using inverse distance weighting, and the spatially distributed values ranged between 65.90 and 155.10 N h^{-1} yr^{-1} across the eight-year study period.

Soil erodibility (K factor) values were computed following {Auerswald, 2014 #156@@author-year} and already provided in the monitoring data set {Auerswald, 2019 #102}. The values, originating from a 50 by 50 m sampling grid, were spatially interpolated using ordinary kriging to generate a continuous surface with a 5 m by 5 m resolution grid. The resulting K factor values across the study area ranged from 1.8 to 4.6 t ha^{-1} h N^{-1}.

The slope length and slope steepness factor (LS factor) was calculated based on the DEM using the approach by {Desmet, 1996 #29@@author-year}. When calculating the LS factor for W01, the shrubbed area (Fig. 1) was excluded due to its negligible runoff contribution. Additionally, we calculated the LS factors for W02 and W03 separately from their upslope catchments (i.e. W01 and W02), since their runoff was directed via underground pipes to the monitoring stations (see Fig. 1).

To account for the temporal dynamics of soil protection, we calculated the C factor based on soil cover and rainfall erosivity. This calculation involved deriving continuous daily soil cover data from field measurements, determining the corresponding soil loss ratios (SLR), and weighting these by the seasonal rainfall erosivity.

From 1994 to April 1997, bi-weekly crop and residue cover measurements were conducted during growing seasons, with monthly measurements during autumn and spring and additional observations before and after soil management operations. To obtain continuous time series, the point data was linearly interpolated to generate daily cover values (Auerswald et al., 2019b). For the subsequent period (April 1997–2001), we applied standardised daily crop development and residue cover curves, which were derived from the daily crop and residue cover values observed during the detailed monitoring phase in combination with management information (mainly sowing and harvest dates) observed between 1997 and 2001 {Auerswald, 2019 #97;Fiener, 2019 #130}. Total soil cover was calculated with residues protecting portions of the otherwise exposed soil according to:

$$Co_{tot} = Co_{crop} + \left(100 - Co_{crop}\right) * \frac{Co_{res}}{100} \quad (2)$$

Where Co_{tot} is the total soil cover (%), Co_{crop} the cover of the growing crop on the respective field (%), and Co_{res} the measured soil cover of the residues (%).

Figure 2 illustrates the total soil cover on the respective fields with monthly rainfall erosivity.

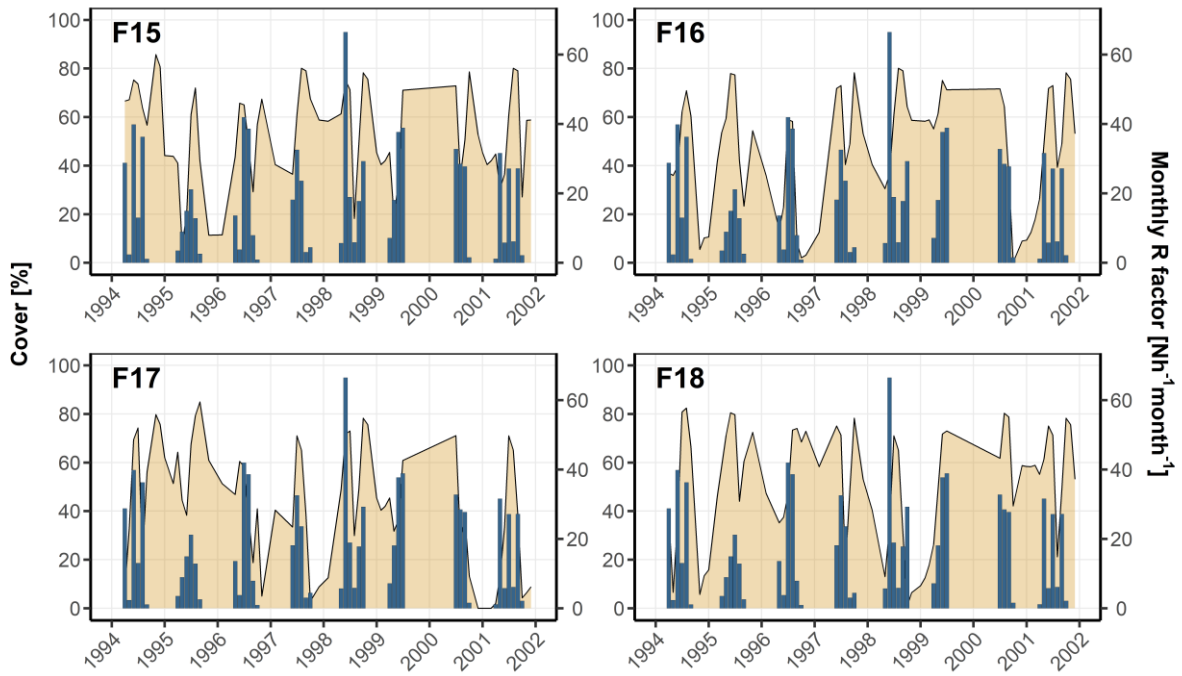

Figure 2: Each field's total soil cover (Residues and crops). Blue bar plots (monthly sum) show monthly R-factors.

The soil loss ratio (*SLR*) quantifies the protective effect of soil cover by comparing potential soil loss under a given vegetation condition to that under standardised fallow conditions {Schwertmann, 1987 #27;Wischmeier, 1978 #17}. While the *SLR* traditionally considers five crop growth stages, from bare soil (0% cover) to full canopy coverage (75-100% cover), we also considered crop residue cover. Determining field-specific *SLR* values involved categorising soil cover into the five growth stages and assigning corresponding *SLR* values. As no-till was applied at the research farm, lower *SLR* values were assigned than in conventional systems due to increased soil surface protection. These *SLR* values were obtained from {Schwertmann, 1987 #27@@author-year} and adapted based on our expert knowledge regarding the soil conservation practices in the Scheyern experimental farm {Fiener, 2007 #93;Fiener, 2019 #130}.~~The annual crop factor (C factor) was calculated by combining seasonal rainfall erosivity with temporal changes in soil coverage {Schwertmann, 1987 #27}. The soil loss ratio (*SLR*) quantifies the protective effect of soil coverage by comparing potential soil loss under a given vegetation condition to that under standardised fallow conditions {Schwertmann, 1987 #27;Wischmeier, 1978 #17}. While the *SLR* traditionally considers five crop growth stages, from bare soil (0% cover) to full canopy coverage (75-100% cover), we also considered crop residue cover.~~

~~From 1994 to April 1997, direct bi-weekly measurements during growing seasons and monthly measurements during autumn and spring were conducted, with additional observations before and after soil management operations. These field measurements included both crop and residue cover. From these field measurements, standardised daily crop development and residue cover were established and used for the subsequent period from April 1997 onwards {!!! INVALID CITATION !!! (Auerswald et al.`, 2019b`; Fiener et al.`, 2019a), #0}.~~

~~Total soil cover was calculated with residues protecting portions of the otherwise exposed soil according to:~~

~~$Co_{tot} = Co_{crop} + \left(100 - Co_{crop}\right) * \frac{Co_{res}}{100}$,~~ ~~(2)~~

~~With Co_{tot} is the total soil cover (%), Co_{crop} the cover of the growing crop on the respective field (%), and Co_{res} the measured soil cover of the residues (%).~~

~~Figure 2 illustrates the total soil cover on the respective fields with monthly rainfall erosivity. Determining field-specific *SLR* values involved categorising soil cover into the five growth stages and assigning corresponding *SLR* values. As no-till was applied at the research farm, lower *SLR* values were assigned than in conventional systems due to increased soil surface protection. These *SLR* values were obtained from {Schwertmann, 1987 #27@@author-year} and adapted based our expert knowledge regarding the soil conservation practices in the Scheyern experimental farm {Fiener, 2007 #93;Fiener, 2019 #130}.~~

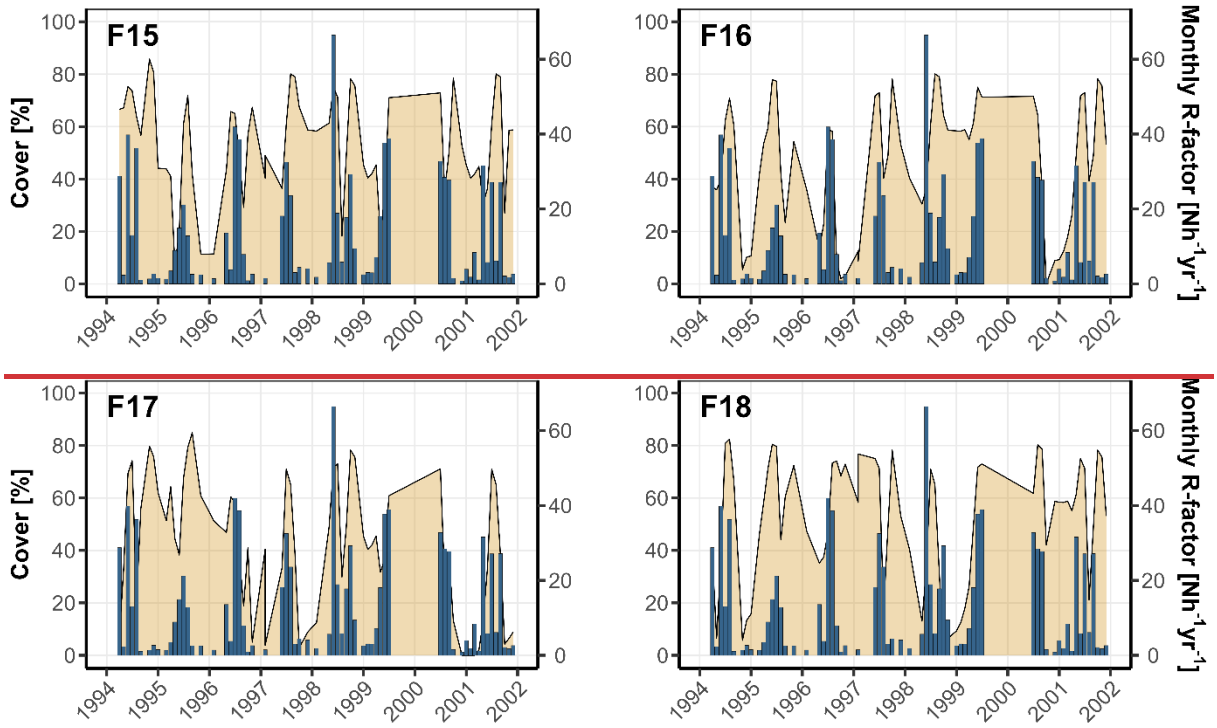

~~**Figure 2: Each field's total soil cover (Residues and crops). Blue bar plots (monthly sum) show monthly R-factors.**~~ The annual C factor was calculated by multiplying the monthly proportion of the R factor with the average *SLR* value of the respective month:

$$C = \sum_{month=1}^{12} SLR_{month} * R_{prop,month} \quad (3)$$

Where C is the cover management factor (dimensionless), SLR_{month} the average soil loss ratio value of the respective month and $R_{prop,month}$ the proportion of the annual rainfall erosivity factor for the respective month (dimensionless).

Figure 3 shows the annual C and R factor throughout the entire study period.

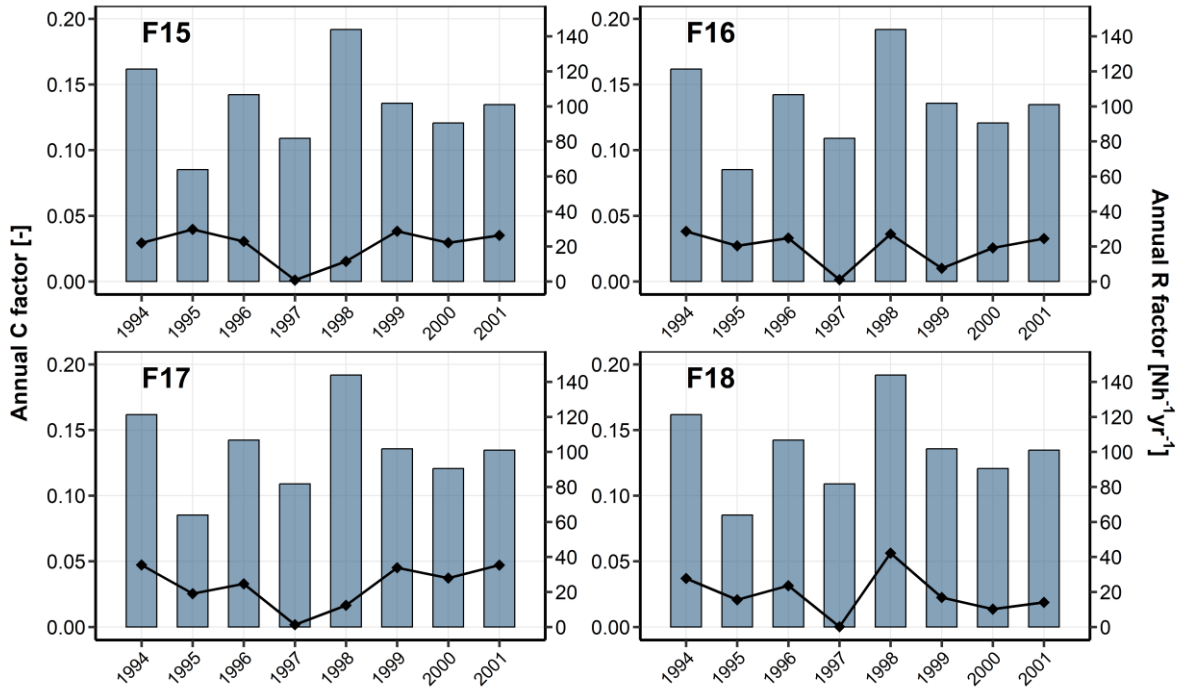

Figure 3: Annual C factor (black dots and lines) and R factor (blue bars) for the individual fields F15 to F18 over eight years.

The support practices factor (P factor) was not specifically parametrised for contour-seeding because of field heterogeneity, i.e. not all parts of a single field were contour-seeded, and/or the absence of specific P factor values for structures such as the potato dams. Furthermore, the field geometries often result in high L factors that often exceed the critical slope length limit for effective contouring defined in the German USLE {Schwertmann, 1987 #27;DIN-Normenausschuss, 2022 #28}. Hence, the effective P-factor converges towards 1.0. W~~However, w~~e accounted for the uncertainty stemming from this lack of parameter representation as part of the model conditioning process (see section 2.4 below).

2.5 Sediment t~~T~~ransport and d~~D~~eposition

~~The~~ Transport c~~C~~apacity (*TC*) quantifies the maximum amount of sediment transported through a grid cell without deposition. When the incoming sediment load into a raster cell exceeds TC, the excess material is deposited within the cell, whilst the remaining portion continues its downstream movement. *TC* was calculated with the approach proposed by {Van Rompaey, 2001 #10@@author-year}:

$$TC = k_{TC} * R * K * (LS - S_{IR}), \quad (4\text{~~3~~})$$

with:

$$S_{IR} = 4.12 * S_m^{0.8} \quad (5\text{~~4~~})$$

where TC is the transport capacity (t ha^{-1}), k_{TC} the transport capacity coefficient (m) described below, R the rainfall erosivity factor in (N h^{-1} yr^{-1}), K is the soil erodibility factor (t ha^{-1} h N^{-1}), LS the slope length and steepness factor (dimensionless), S_{IR} the interrill slope gradient factor (dimensionless) and S_m the slope (m m^{-1}).

The transport capacity coefficient (k_{TC}) represents the theoretical upslope distance required for sediment generation to reach maximum *TC* at a given raster cell under the assumption of uniform slope and erosion conditions {Van Rompaey, 2001 #10}. The transport capacity coefficient depends on surface roughness and therefore differs according to land use and management. In our model parameterisation, we distinguish between higher values for arable land ($k_{TC/A}$) and lower values for grassland ($k_{TC/G}$; along field borders and in grassed waterways), which were subjected to the GLUE-based analysis (see Section 2.7).~~In our model parameterisation, we distinguish between higher values for arable land ($k_{TC/A}$) land and lower values for grassland ($k_{TC/G}$; along field borders and in grassed waterways).~~

WaTEM/SEDEM's hillslope sediment transport module employs a multiple flow routing algorithm, which distributes sediment from individual cells to their downslope neighbours based on {Quinn, 1991 #32@@author-year}. The algorithm calculates local slopes to eight neighbouring cells and applies specific weighting factors: 0.50 for orthogonal neighbours and 0.35 for diagonal neighbours. The sediment flux is distributed proportionally to the weighted slope values of all cells at equal or lower elevations.

In this study, we implemented the p~~P~~arcel c~~C~~onnectivity (p_{con}) parameter specifically at field boundaries. p_{con} reduces the contributing upstream area by a value [%] at these transitions {Notebaert, 2006 #76}. This reduction has a dual effect: (i) it directly lowers the slope length part of the LS factor, thereby decreasing the potential erosion for subsequent downstream cells, and (ii) it affects ~~the~~ TC, which is calculated using the LS factor (Eq. 4~~3~~). Unlike the original WaTEM/SEDEM version {Notebaert, 2006 #76}, we implemented p_{con} within the multiple flow routing algorithm loop calculating the contributing upstream area, ensuring its effects propagate downstream through the flow network. Consequently, the reduction in sediment transport influences the downstream cells and extends to subsequent agricultural fields and vegetated areas. Moreover, we introduced a border deposition (b_{dep}) parameter, which represents a forced deposition mechanism activated when agricultural field cells contribute sediment to adjacent vegetated areas. Under these conditions, a defined percentage of the transported sediment is deposited directly at the field border within the field.

Retention ponds were implemented within the 5 m by 5 m land use raster map. The locations of the four retention ponds at the outlets of the micro-scale watersheds were mapped, with assigned trapping efficiencies of 54~~–~~%, 82 %, 59~~–~~%, and 85~~–~~% for watersheds W01, W02, W05, and W06, respectively, as measured in {Fiener, 2005 #155@@author-year}. The standard deviation across all watersheds (± 14%) was applied to account for measurement error in the trapping efficiency values within the GLUE framework (see Section 2.6).~~The standard deviation across all watersheds (± 13.7 %) was applied to account for measurement error in the trapping efficiency values~~.

2.6 Generalised Likelihood Uncertainty Estimation (GLUE)~~ framework~~

We employed the GLUE methodology {Beven, 1992 #129} to represent model and measurement uncertainties and to identify and analyse behavioural parameter spacesets. The GLUE approach recognises that multiple parameter sets may provide equally acceptable simulations of a system within the limitations of a given model structure and observational errors {Beven, 2006 #125}.

We established limits of acceptability for the simulated sediment yields by considering multiple sources of uncertainty in the event-based measurements of runoff and sediment concentrations used for calculating annual and ~~median~~ mean annual sediment yields. These included Coshocton wheel measurement errors {± 10%`, \Fiener, 2003 #124}, runoff collector ~~barrel~~ storage tank sampling errors (estimated ± 10 ~~–~~%), and retention pond uncertainties (± 14 %). For events with data collection issues (flagged in the data set), we assigned an additional ± 50 % error margin. However, for events flagged as "~~barrels~~ storage tank overflown", we introduced only an upper error boundary since the measurement taken from the ~~barrel~~ storage tank represents a minimum possible sediment yield during a rainfall event. Finally, we propagated the measurement errors using a Monte Carlo simulation with 1,000 realisations and sampling from normal distributions that represented the range of potential errors. The 2.5th and 97.5th percentiles of the resulting aggregated (annual and mean ~~median~~ annual) sediment yields were used as the limits of acceptability for simulated values. These uncertainty bounds served as criterion for identifying behavioural model realisations. Hence, only simulations producing outputs within these error margins were classified as behavioural and retained for subsequent analysis.

2.7 Model conditioning and evaluation

The model results were evaluated using R-Studio (R 4.4.2; R-Studio 2024.12.1 Build 563) in two phases to account for the different sediment transport processes in field-dominated and structure-dominated watersheds.

Phase 1 - Field-dominated watersheds:

We performed a Monte Carlo simulation with 25,000 realisations for the field-dominated watersheds, sampling parameters from uniform distributions across *a priori* selected ranges (Tab. 1). To consider the inherent potential errors in USLE calculations, including uncertainties associated with the parameterisation of the P factor, we modified the potential erosion in individual raster cells through an error surface (e_{sur}) before routing the sediment. This error surface was sampled from a uniform distribution for each realisation, modifying the USLE-calculated potential erosion (Eq. 1) within a range of 0 to ± 0.5:

$$A_{new,i} = A_i + A_i * e_{sur}, \quad (6\sout{5})$$

Where A_i is the potential soil erosion (t ha^{-1} yr^{-1}) calculated by the USLE (Eq. 1) at raster cell i, $A_{new,i}$ is the potential soil erosion (t ha^{-1} yr^{-1}) with incorporated uncertainty at raster cell i, and e_{sur} the error surface (dimensionless).

The decision to aggregate the uncertainty of the ABAG factors into a single error surface (e_{sur}), rather than sampling individual factors within the Monte Carlo simulation, stemmed from the nature of our input data. We assumed that parameterisation errors (apart from the P factor) were negligible due to the exceptionally high-quality monitoring data used as input for calculating the ABAG factors (section 2.4). However, as the ABAG is based on regressions that carry residual error, we pragmatically used an error surface to evaluate inherent model biases.

To ensure that $k_{TC/G}$ is consistently lower than $k_{TC/A}$, both were sampled with a constrained relationship, where $k_{TC/A}$ values were required to be at least 1.5 but no more than 5 times higher than $k_{TC/G}$ values. Model realisations

~~runs~~ were classified as behavioural if the simulated sediment yield values fell within the established limits of acceptability (error margins) for the observed data. Likelihoods were calculated only for the spatiotemporal aggregated data for which behavioural model realisations were identified. For these behavioural simulations, we calculated likelihoods by rescaling the mean absolute error (*MAE*) {Brazier, 2000 #70}:

$$L_i = \frac{1}{MAE_i} / \sum \frac{1}{MAE_i}, \quad (7\text{~~6~~})$$

with:

$$MAE_i = |Sim_i - Obs_i|, \quad (8\text{~~7~~})$$

where L_i is the likelihood of one realisation i (dimensionless), MAE_i is the mean absolute error of realisation i (t ha^{-1} yr^{-1}), Sim_i is the simulated values for behavioural runs of realisation i (t ha^{-1} yr^{-1}), and Obs_i is the observed sediment value for realisation i (t ha^{-1} yr^{-1}).

Table 1: Parameter ranges used for MC simulation in the WaTEM/SEDEM model. These ranges were selected based on the literature on previous model applications. $k_{TC/A}$ and $k_{TC/G}$ are the transport capacity coefficients for arable land and grassland, p_{con} is the parcel connectivity, e_{sur} is the error surface and b_{dep} the border deposition.

Range	$k_{TC/A}$ [m]	$k_{TC/G}$ [m]	p_{con} [%]	e_{sur}	b_{dep} [%]
low	1	1	50	-0.5	0
high	300	100	90	0.5	20

Phase 2 - Structure-dominated watersheds:

For the structure-dominated watersheds, we used the likelihoods associated with behavioural parameter values conditioned in Phase 1 to represent in-field processes ($k_{TC/A}$ and e_{sur}) in order to generate another ~~model~~ 25,000 realisations. In this second phase, ~~the~~ model conditioning was focused on the parameters controlling sediment redistribution through landscape structures ($k_{TC/G}$, b_{dep} and p_{con}). The same limits of acceptability approach as in phase one was applied to identify behavioural simulations. We calculated new likelihood values for these simulations to analyse their performance in representing structural erosion control practices~~measures~~.

2.8 Spatiotemporal model evaluation

Model outputs were ~~analysed~~ evaluated at multiple spatiotemporal scales through sequential aggregation steps to analyse short-term dynamics against its intended long-term design: First, we~~we calculated an eight-year~~temporally aggregated the sediment yields by calculating eight-year means ~~median of the sediment yield~~ for each individual watershed. Second, we spatially aggregated the simulated sediment yields by calculating their means for each watershed group (field- and structure-dominated), but keeping an annual resolution. ~~Second, we spatially aggregated the watersheds based on their dominant erosion characteristics (field- and structure-dominated) while maintaining an annual resolution.~~ Third, eight-year means for each watershed group were calculated (spatial and temporal aggregation)~~we aggregated the median values over the eight-year monitoring period for these spatially aggregated groups~~.

To further analyse relative errors, the percent bias ($PBIAS$) was calculated by:

$$PBIAS = \left(\frac{Sim_i - Obs_i}{Obs_i}\right) * 100, \quad (98)$$

Where Sim_i is the simulated values for behavioural realisation i (t ha^{-1} yr^{-1}), and Obs_i is the observed sediment value for realisation i (t ha^{-1} yr^{-1}).

2.9 Spatial analysis

Spatial analysis was performed using R-Studio (R 4.4.2; R-Studio 2024.12.1 Build 563). To quantify the spatial distribution of sediment yield and the associated uncertainty, the cell-wise mean and standard deviation were calculated across all behavioural model realisations.

3. Results

3.1 Model pPerformance aAcross sScales

The modelled annual sediment yields ~~model results~~ for field-dominated watersheds (W01-W04) were within the same order of magnitude of the measurements~~d sediment yields~~. However, the model was not considered behavioural for predicting annual sediment yields according to our pre-established acceptability criterion. The simulated annual sediment yields were predominantly overestimated (22 out of 32 cases; Fig. 4~~3~~a-d), occasionally underestimated (~~3~~4 out of 32 cases~~;, i.e.~~ in the year 1997 and 2000 in W01; 1994 in W02; 1994 in W04; Fig. 4~~3~~a, b and d), with only a small portion of simulations ~~meeting our acceptability criterion~~overlapping the observational data (6~~7~~ out of 32 cases; Fig. 4~~3~~a-d). The tendency to overestimate sediment yield is more pronounced in watersheds W05 and W06. Only in 1994 the model had the tendency to underestimate~~d~~ measured sediment yields in watershed W05 (Fig. 5~~4~~b). In W06, measured sediment yields were the lowest among all watersheds (maximum of 0.02 t ha^{-1} yr^{-1} in 2000), with zero sediment yield measurements in 1995, 1997, and 2001, yet the model consistently overestimated sediment yield across all years in this watershed.

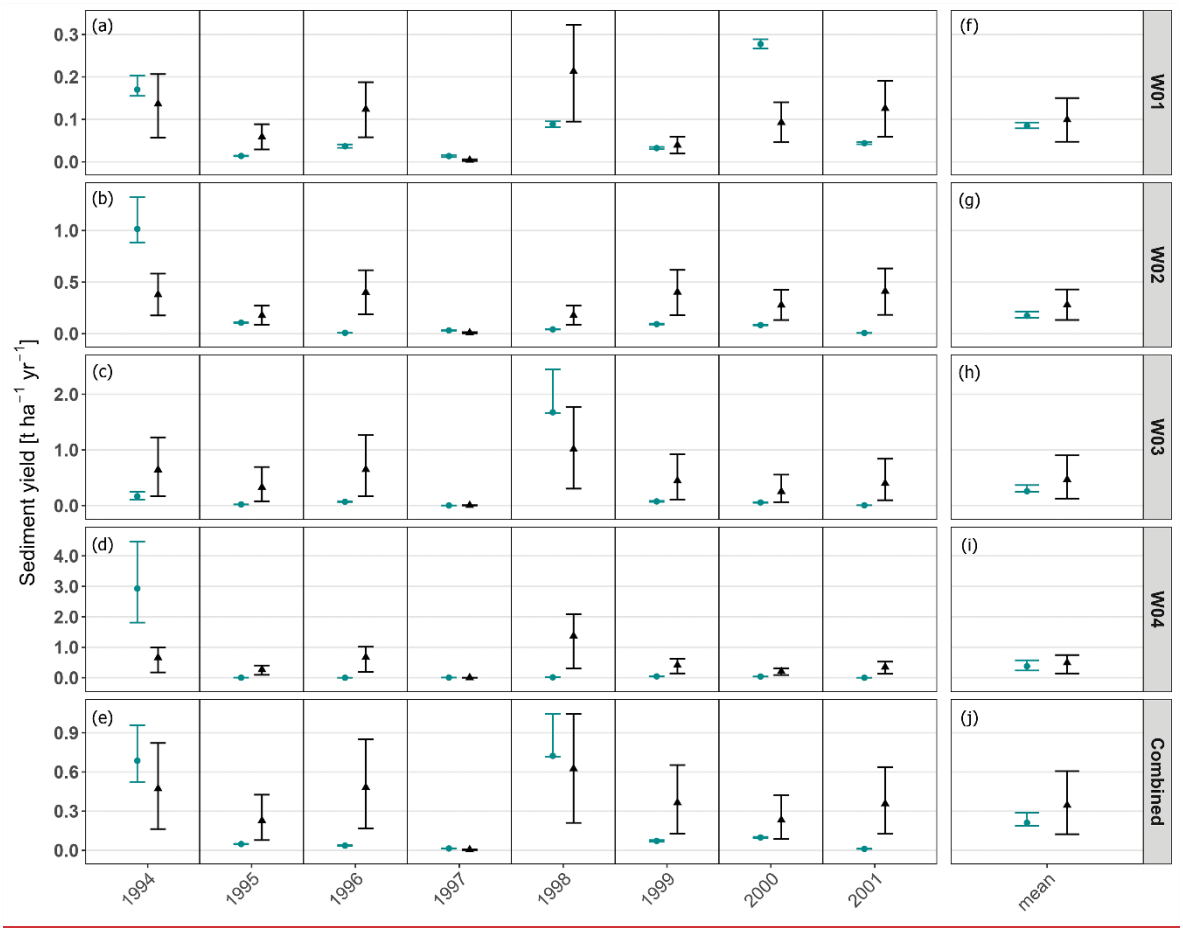
Sediment yield [t ha^{-1} yr^{-1}]
(a)
(b)
(c)
(d)
(e)
(f)
(g)
(h)
(i)
(j)
W01
W02
W03
W04
Combined
1994
1995
1996
1997
1998
1999
2000
2001
mean

474

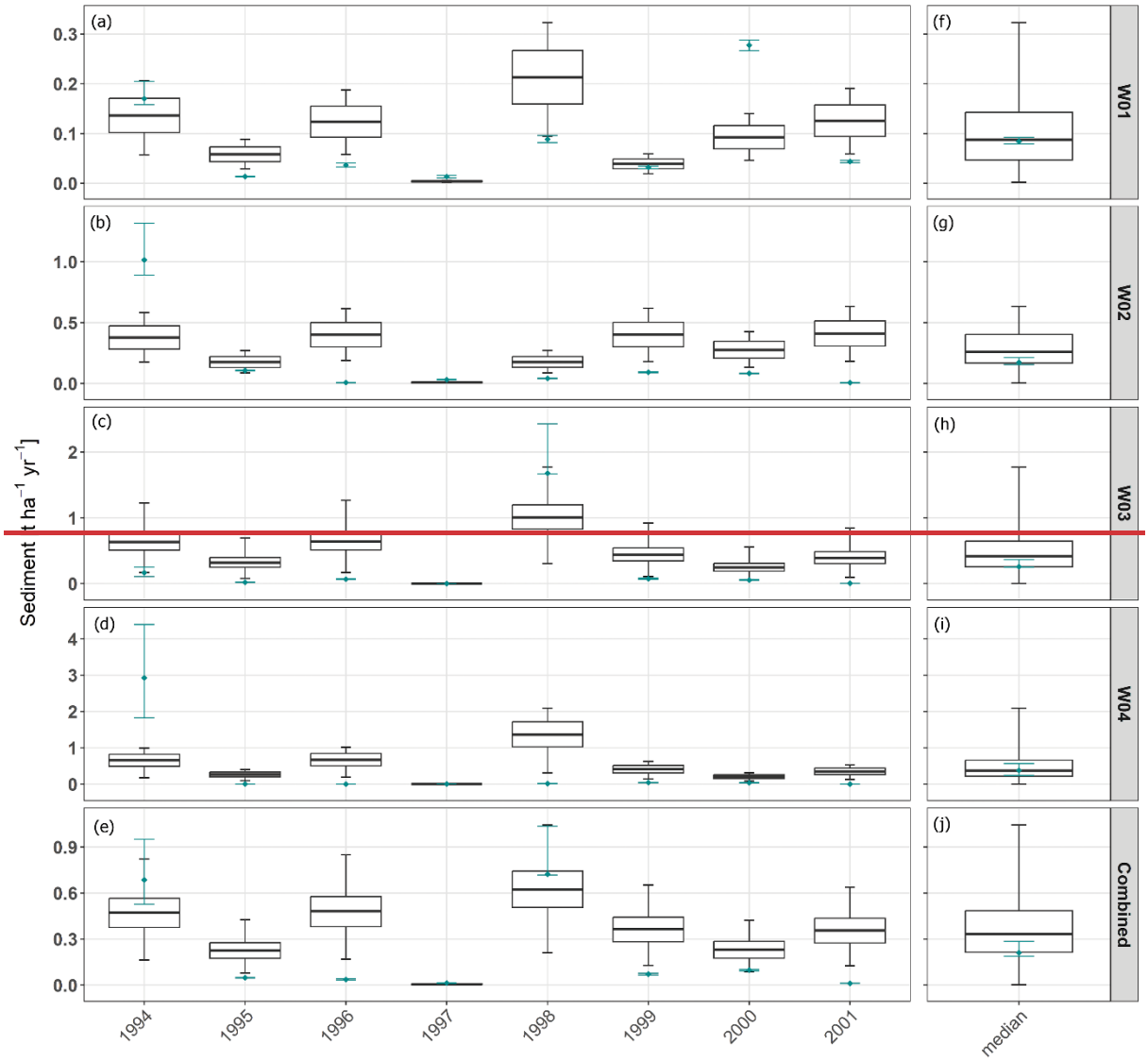

Figure ~~13~~ 12: Annual and eight-year~~s~~ mean ~~median~~ sediment yields in field-dominated watersheds. (a-d) Annual sediment yields: ~~Box plots display the median, 1. and 3. quartile and the full range of simulated sediment yields~~Black triangles indicate the mean and the full range from 25,000 model realisations ~~with different parameter sets~~ (black whiskers), while cyan dots represent mean measured sediment yields with computed error ranges (cyan whiskers)~~while median sediment yield measurements are shown as blue dots with computed error ranges (cyan whiskers)~~. (f-i) The watershed-specific eight~~8~~-year mean measured sediment yields (cyan~~median measured yield with error ranges)~~ ~~and~~and eight-year mean simulated yields (black). (e) Spatially combined annual watershed sediment yields.~~Annual spatially combined watershed sediment yields.~~ (j) Spatially aggregated eight-year mean yields~~8-year median of spatially aggregated watersheds~~. Note: In some years (e.g., 1998), cyan whiskers show larger uncertainties above the mean values; this is because storage tank overflow contributes only to higher uncertainties (see Section 2.6).

When evaluated using eight-year mean ~~median~~ values per watershed, ~~model performance~~simulations showed better agreement with observations. The temporal aggregation revealed varying proportions of behavioural model realisations across individual watersheds. W04 had the highest amount with 69 % of all realisations, while other watersheds exhibited lower proportions (W01: 13 %, W02: 22 %, W03: 22 %). W05 exhibited minimal behavioural realisations of 1 %. In W06 (Fig. 5c), none of the actual model realisations matched the observational data including measurement errors. Furthermore, no common behavioural realisations were found across all watersheds, indicating that each watershed had a different behavioural parameter space. The analysis of the spatially aggregated watersheds (field-dominated vs. structure-dominated), while maintaining annual temporal

resolution, revealed behavioural model realisations in some years but not consistently throughout the entire eight-year period for each watershed group (Fig. 4e, 4b).

~~The eight-year median modelled sediment yield across field-dominated watersheds (W01-W04) was 0.24 t ha^{-1} yr^{-1}, closely aligning with the measured eight-year median of 0.21 t ha^{-1} yr^{-1}. For structure-dominated watersheds W05 and W06, we simulated an eight-year median of 0.15 t ha^{-1} yr^{-1} (Fig. 4c, d), against a measured median of 0.13 t ha^{-1} yr^{-1}. The 1994 sediment yield peak in W05 strongly influenced the system's overall performance, ultimately leading to an increased number of behavioural model realisations when evaluated across the entire period (Fig. 4d).~~

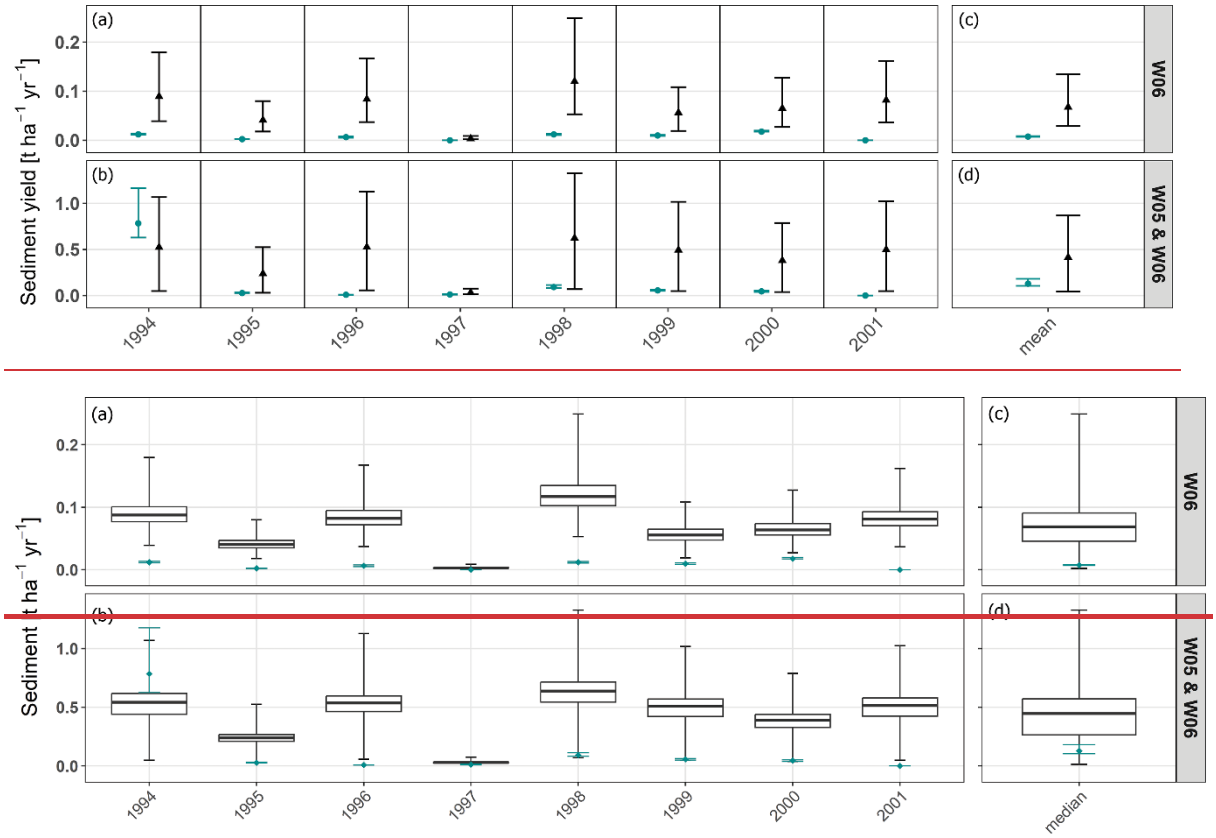

Figure 5~~4~~:~~-~~ Annual and eight-year mean sediment yields in ~~Annual and eight-years median sediment yields in~~ structure-dominated watersheds. (a-b) Annual sediment yields: Black triangles indicate the mean and the full range from 25,000 model realisations (black whiskers), while cyan dots represent mean measured sediment yields with computed error ranges (cyan whiskers). ~~Box plots display the median, 1. and 3. quartile and the full range of simulated sediment yields from 25,000 model realisations with different parameter sets (black whiskers), while median sediment yield measurements are shown as blue dots with computed error ranges (cyan whiskers).~~ **(c-d)** The watershed-specific eight-year mean measured sediment yields (cyan) and eight-year mean simulated yields (black).~~The watershed-specific 8-year median measured yield with error ranges and simulated yields.~~

When combining both spatial and temporal aggregation, behavioural realisations were generated for each watershed group (Fig. 4j, 5d). Across the entire set of 25,000 realisations, the mean *MAE* values were 0.14 t ha^{-1} yr^{-1} for field-dominated watersheds and 0.29 t ha^{-1} yr^{-1} for structure-dominated watersheds, with maximum *MAE* values of 0.40 t ha^{-1} yr^{-1} and 0.74 t ha^{-1} yr^{-1}, respectively. Table 4 presents the model performance metrics specifically for the subset of behavioural model realisations within the watershed groups. The eight-year mean modelled sediment yield across field-dominated watersheds (W01-W04) was 0.35 t ha^{-1} yr^{-1}, compared to the

measured eight-year mean of 0.21 t ha^{-1} yr^{-1}. For structure-dominated watersheds W05 and W06, we simulated an eight-year mean of 0.41 t ha^{-1} yr^{-1} (Fig. 5c, d), against a measured mean of 0.13 t ha^{-1} yr^{-1}. The 1994 sediment yield peak in W05 strongly influenced the system's overall performance, ultimately leading to an increased number of behavioural model realisations when evaluated across the entire period (Fig. 5d).

~~The eight-year temporal aggregation revealed varying proportions of behavioural model realisations across individual watersheds. W04 had the highest amount with 57 % of all realisations, while other watersheds exhibited lower proportions (W01: 13 %, W02: 21 %, W03: 23 %). W05 exhibited minimal behavioural realisations of 1 %. Although the range of our simulated values overlapped with the error margins for the measured sediment yields in W06 (Fig. 4c), none of the actual model realisations matched the observational data including measurement errors. Furthermore, no common behavioural realisations were found across all watersheds, indicating that each watershed had a different behavioural parameter space.~~

~~The analysis of the spatially aggregated watersheds (field-dominated vs. structure-dominated), while maintaining annual temporal resolution, revealed behavioural model realisations in some years but not consistently throughout the entire eight-year period for each watershed group (Fig. 3e, 4b). When combining both spatial and temporal aggregation, behavioural realisations were generated for each watershed group (Fig. 3j, 4d). Across the entire set of 25,000 realisations, the median *MAE* values were 0.12 t ha^{-1} yr^{-1} for field-dominated watersheds and 0.16 t ha^{-1} yr^{-1} for structure-dominated watersheds, with maximum *MAE* values of 0.34 t ha^{-1} yr^{-1} and 0.39 t ha^{-1} yr^{-1}, respectively. Table 4 presents the model performance metrics specifically for the subset of behavioural model realisations within the watershed groups.~~

Table 2: Comparison of model performance metrics between micro-scale watershed groups based on eight-year mean ~~median~~ of behavioural realisations, including mean ~~median~~ sediment yield (SY) as well as error statistics (MAE, PBIAS) with maximum (Max.), ~~, median (Med.) and~~ minimum (Min.) and mean values.

Unit of measure		Field-dominated	Structure-dominated
Behavioural realisations [%]		~~30.04~~28.70	1.3~~53~~
Measured SY [t ha^{-1} yr^{-1}]	Mean~~d~~	0.21	0.13
Simulated SY [t ha^{-1} yr^{-1}]	Mean~~d~~	0.24	0.15
MAE [t ha^{-1} yr^{-1}]	Min.	4.21*10^{-6}	5.76*10^{-5}
	Mean~~d~~	0.0~~43~~	0.03
	Max.	0.0~~87~~	0.05
PBIAS	Min.	-11.51~~0.79~~	-17.70

[%]	Meand	15.1935	20.1515.96
	Max.	36.695.38	42.2964

3.2 Behavioural parameter space

We analysed the behavioural parameter space for the spatially and temporally aggregated watershed groupsmodel outputs, as only this aggregation level yielded behavioural realisations for both field-dominated and structure-dominated watershed groups.

For field-dominated watersheds, the analysis focused on the error surface and in-field parameter e_{sur} and $k_{TC/A}$. While behavioural realisations were identified across the entire ranges of all parameters, higher likelihood values concentrated in specific regions. Specifically, e_{sur} values closer to -0.5 exhibited higher likelihood values than lower e_{sur} values (Fig. 65b). In contrast, $k_{TC/A}$ showed no discernible pattern across the response surface (Fig. 65c). The relationship between these parameters revealed a clear compensation mechanism, where lower $k_{TC/A}$ values required higher e_{sur} s_{cor} values to produce behavioural realisations (Fig. 65a).

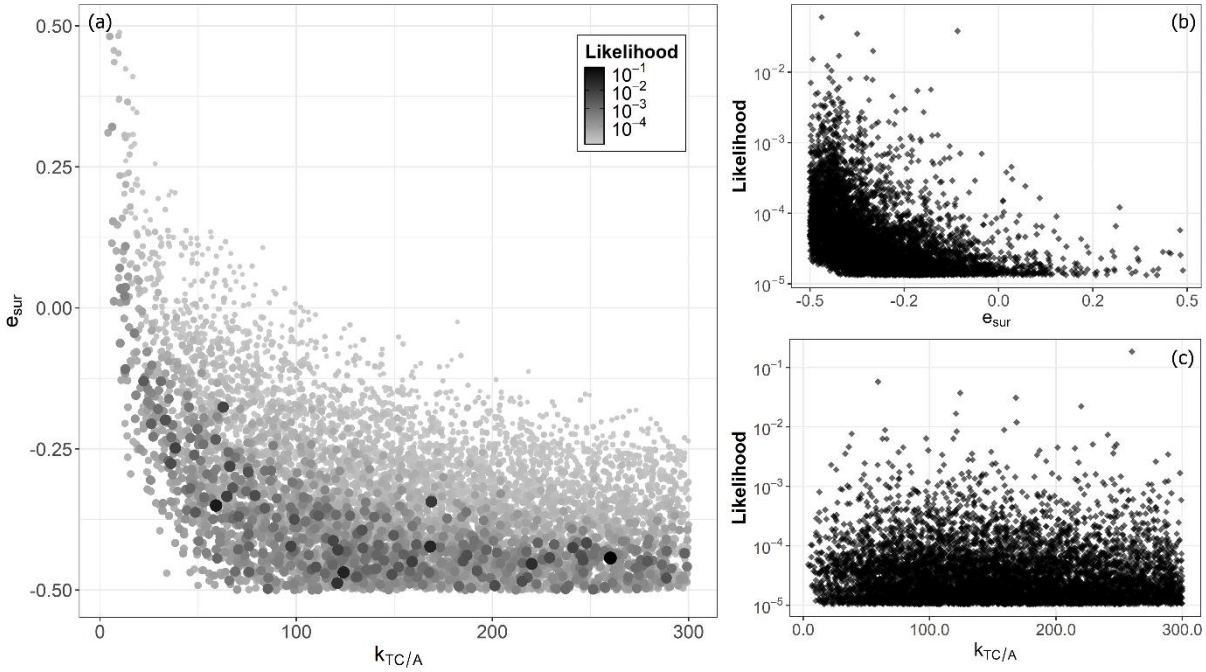

Figure 65: Parameter likelihoods across field-dominated micro-scale watersheds, showing only behavioural model realisations. (a) The relationship between e_{sur} and $k_{TC/A}$ parameters. Circle size and shade intensity indicate the likelihood of each parameter combination, with larger and darker circles representing higher likelihood values. (b) The relationship between likelihood and e_{sur}. (c) The relationship between likelihood and $k_{TC/A}$.

In structure-dominated watersheds, the analysis focused on parameters controlling sediment transportation and deposition in grasslands and landscape structures ($k_{TC/G}$, b_{dep}, and p_{con}). The $k_{TC/G}$ parameter exhibited a distinct likelihood peak between approximately 9 and 11 m, with behavioural values ranging from approximately 7.5 m to 15 m (Fig. 76a), which is notably narrower than the sampled range of up to 150 (Tab. 1). In contrast, b_{dep} and p_{con} showed no sensitivity, displayingdisplayed relatively uniform likelihood distributions across their entire ranges (Fig. 76b, c). When plotting b_{dep} against p_{con}, homogeneous likelihood distributions emerged with no apparent

dependencies (Fig. 7~~6~~f). Examinations of b_{dep} and p_{con} against $k_{TC/G}$ revealed a horizontal band of high likelihood values at specific $k_{TC/G}$ values, without any directional trends (Fig. 7~~6~~d, e).

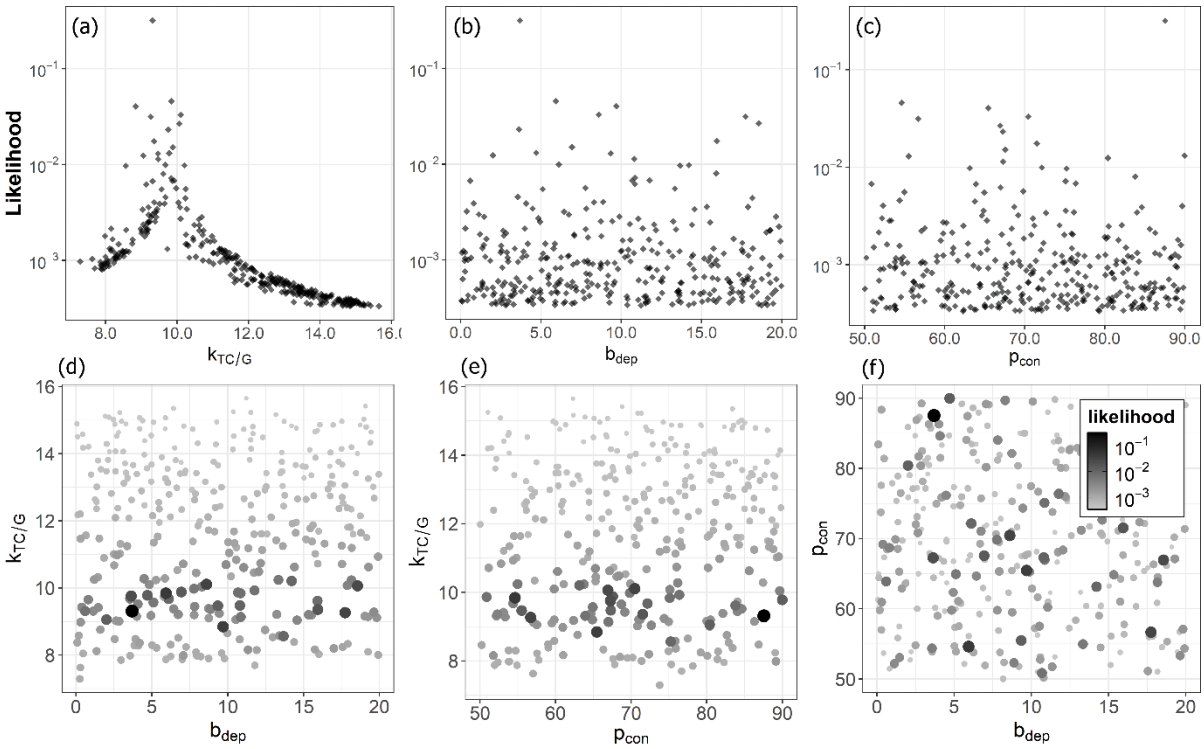

Figure 7~~6~~: Parameter likelihoods across structure-dominated micro-scale watersheds, showing only behavioural model realisations. (a) The relationship between likelihood and $k_{TC/G}$. (b) The relationship between likelihood and b_{dep}. (c) The relationship between likelihood and p_{con}. (d) The relationship between b_{dep} and $k_{TC/G}$. Circle size and colour intensity indicate the likelihood of each parameter combination, with larger and darker circles representing higher likelihood values. (e) The relationship between p_{con} and $k_{TC/G}$. (f) The relationship between b_{dep} and $k_{TC/G}$.

3.3 Spatial analysis

In field-dominated watersheds, substantial deposition was primarily confined to retention ponds, while other areas outside arable lands showed ~~relatively~~ minimal deposition, except for W03 (Fig. 8a). ~~, as shown in the 50th percentile (median) of behavioural model realisations (Fig. 7a).~~ In W04, negligible to no deposition was observed. Conversely, structure-dominated watersheds exhibited considerably more intense erosion-deposition dynamics. The grassed waterway showed a clear deposition pattern, with W06 exhibiting the most pronounced deposition patterns leading toward the retention pond at the outlet ~~of W06~~.

The map of the standard deviation (Fig. 8b) also displays a spatial shift in model uncertainty between the two watershed groups. In field-dominated watersheds, standard deviation exhibits concentrations along in-field flow pathways, the retention ponds and the small structures next to their outlets. In structure-dominated watersheds

a substantial increase in standard deviation is visible along the flow pathways towards and along the grassed waterway.

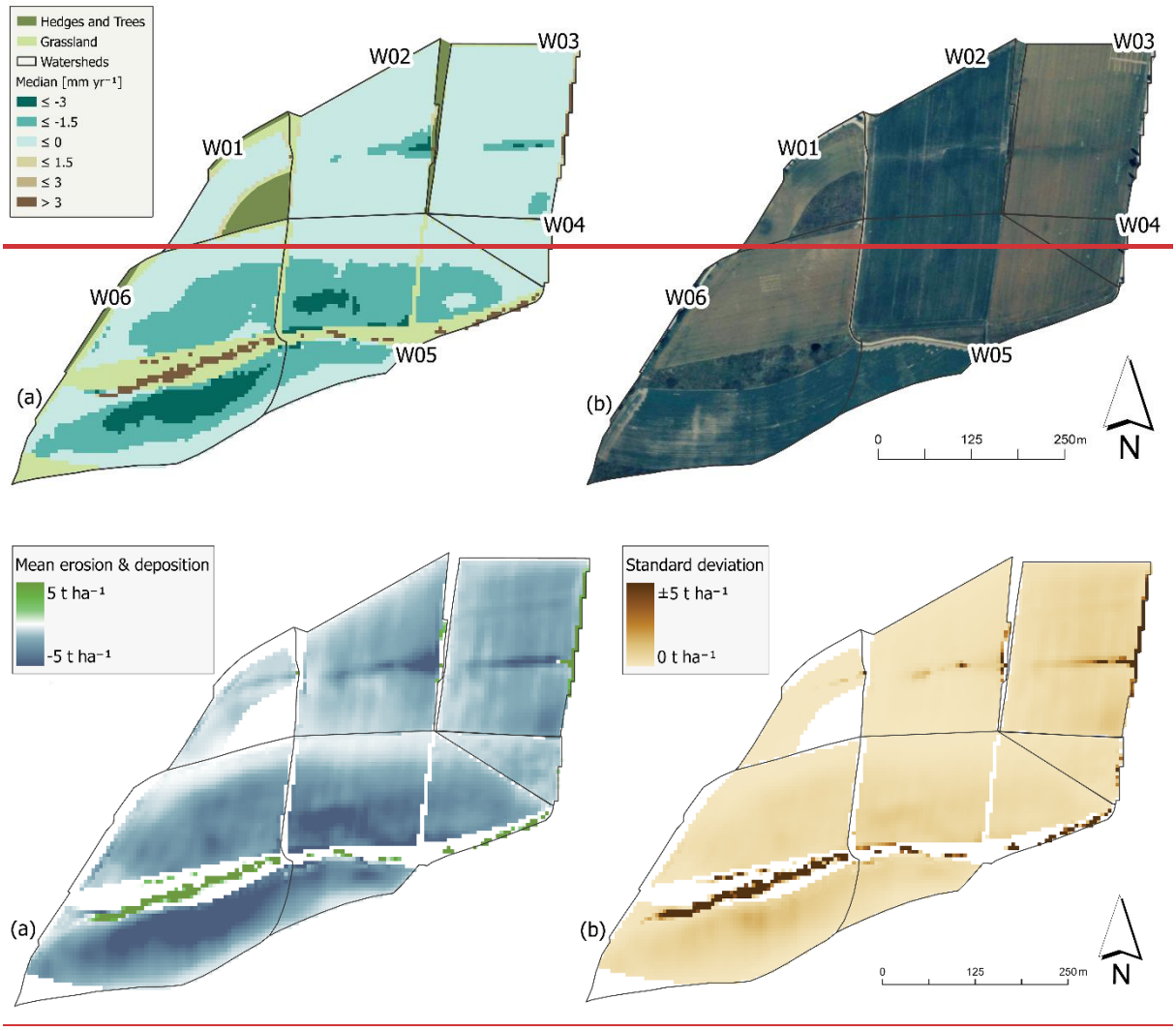

Figure 8~~7~~: (a) The ~~median~~ mean of simulated potential erosion and deposition of behavioural model realisations over the eight-year period. Negative values indicate erosion and positive values deposition. (b) The cell-wise standard deviation of behavioural model realisations over the eight-year period. ~~(b) An aerial photograph of the study area shows the land use patterns and field boundaries on the Scheyern experimental farm in 2002.~~

4. Discussion

4.1 GLUE f~~F~~ramework and u~~U~~ncertainties

We tested WaTEM/SEDEM using a limits of acceptability approach within the GLUE framework. For this, we implemented a two-phase ~~approach~~procedure, first conditioning and evaluating field-dominated watersheds, and then using the behavioural parameter space of these watersheds to condition and evaluate structure-dominated systems. {Alatorre, 2010 #123@@author-year} demonstrated that soil erosion models often exhibit parameter compensation effects, where different parameter combinations produce similar outputs at the catchment scale - a manifestation of the equifinality concept {Beven, 2006 #125}. Our sequential approach helped

to minimise these effects by first constraining the simulated erosion ($k_{TC/A}$ and e_{sur}) in field-dominated watersheds and then conditioning the transport parameters ($k_{TC/G}$, p_{con} and b_{dep}) in more complex systems.

The limits of acceptability approach incorporated multiple sources of measurement uncertainty. {Nearing, 2000 #153@@author-year} demonstrated through replicated plot studies that natural variability in erosion measurements is particularly pronounced for low-magnitude erosion events, such as the ones observed in this study. While {Nearing, 2000 #153@@author-year} proposed a quantitative method for estimating the expected variability of erosion measurements, his approach is specifically developed for plot-scale studies and cannot be extrapolated to watersheds or more complex landscape systems. Given the (to the best of our knowledge) current absence of methodologies for determining error boundaries for low sediment yield measurements at larger scales, we necessarily relied on relative error estimates. An implementation of proper measurement variability-derived error ranges would likely result in a substantially higher number of behavioural model realisations, particularly for low sediment yield measurements where the variability is the highest {Nearing, 2000 #153}. This reveals the need for developing robust approaches for defining limits-of-acceptability criteria for sediment yield estimates that account for the full range of uncertainties, e.g. instrument precision, sampling errors, data processing, or site-specific variations.

Erosion models typically exhibit systematic biases, overpredicting low sediment yields while underpredicting high sediment yields {Nearing, 1998 #134;Risse, 1993 #34;Kinnell, 2007 #83}. This is particularly relevant for our study area, where the implemented watershed-wide soil conservation and sediment trapping resulted in a measured mean sediment yield of only~~the median measured sediment yield of~~ 0.16 t ha^{-1} yr^{-1}~~,~~, which is substantially lower than erosion rates typically range between 3-10 t ha^{-1} yr^{-1} ~~was substantially lower than erosion rates which can exceed 10 t ha^{-1} yr^{-1}~~ in the Bavarian Tertiary hill region {Auerswald, 2009 #137}. To investigate the modelling under/over prediction issue, we used an error surface (e_{sur}) multiplied with the erosion calculated by the USLE (Eq. 6~~5~~). ~~The e_{sur} parameter served three purposes: (i) adjusting potential erosion to investigate the USLE's inherent biases, (ii) analysing the biases by looking at the behaviour of e_{sur}, and (iii) representing the uncertainty stemming from measurement errors for the USLE factors and the lack of parameterisation for the P factor.~~ The analysis of behavioural model realisations revealed a concentration of likelihood values near small e_{sur} values, reducing sediment by up to 50 % (Fig. 6~~5~~b). This indicates that in our study WaTEM/SEDEM overestimates soil erosion in landscapes with implemented conservation practices~~measures~~. This is also evident looking at figure 3a-d and 4a-b, which illustrate a general tendency for overestimation of modelled sediment yields in all watersheds.

4.2 Model p~~P~~erformance and l~~L~~imitations

WaTEM/SEDEM correctly simulated the magnitude of the very low sediment yields in micro-scale watersheds optimised for soil conservation and reduced sediment transport~~under optimized soil conservation~~, with annual values closely aligning with measured data (Fig. 4~~3~~a-d, 5~~4~~a-b). Nonetheless~~Despite this achievement~~, the model did not consistently meet our ~~strict~~ limits of acceptability for annual realisations and therefore was rejected for making precise annual simulations. T~~However, t~~he model's performance improved notably when applied to longer-term means ~~medians~~ and larger spatial units, where more behavioural model realisations were identified.

Field-dominated watersheds

The model simulated the very low sediment yields resulting from well-established in-field soil conservation practices in field-dominated watersheds, comparable to the measured data. In general, observed sediment yields were overestimated, which can be attributed primarily to difficulties in accurately representing ~~the specific C factors of~~ this conservation system, particularly unique practices such as mustard sown onto autumn-built dams where potatoes were later directly planted {Fiener, 2003 #124}. Such unconventional approaches are not adequately captured in the *SLR* values for no-till systems as evaluated in the German adaptation of the USLE {ABAG`; \Schwertmann, 1987 #27;NAW, 2022 #132}, even with the use of very low soil loss ratios in the parameterisation of the C factor, which represent the continuous soil cover through the crop rotation in the experimental farm (Fig. 2).

Conversely, the model underestimated sediment yields in some years because even optimally managed conservation systems experience short time windows with weak protection. During these short windows with reduced soil protection (Fig. 2), substantial erosion events may occur, like in systems not under soil conservation. In general, erosion processes are typically dominated by extreme events {Gonzalez-Hidalgo, 2012 #126;Steegen, 2000 #78}, as exemplified in our study by an April 1994 rainfall event of 114 mm within 66 hours coinciding with low soil coverage in W02 (Fig. 2), accounting for approximately 58 % of that year's total sediment yield (see year 1994 in Fig. 4~~3~~b). The model's annual time step fails to capture these critical temporal coincidences, a structural limitation that becomes more pronounced when such events are infrequent. This temporal limitation aligns with findings by {Risse, 1993 #34@@author-year}, who demonstrated that USLE's model efficiency diminishes at the annual scale. When averaging over the eight-year study period, these extreme events are smoothed out, which explains the model's improved performance at longer timescales (Tab. 2). ~~This observation supports the basic assertion that the USLE was designed to compute long-term soil losses (Wischmeier and Smith 1978).~~

This deficit could not be compensated using high-resolution input data (daily soil cover, high resolution and on-site rainfall measurements). ~~{Srikanthan, 2001 #186}~~However, it is important to note that the episodic nature of erosion is always difficult to capture even with event-based models, and hence aggregation over time tends to improve any kind of erosion model. This is especially true if events are rare and the overall erosion values are small {Nearing, 1998 #134}. Future studies could employ synthetic data generation {e.g. stochastic climate simulation; \Srikanthan, 2001 #186}, allowing for an assessment of the model's sensitivity beyond our high-resolution input data.

For the temporally aggregated eight-year means~~medians~~, there was no single parameter set that produced behavioural model realisations across all field-dominated watersheds simultaneously when applying our limits of acceptability criterion. This indicates a limitation in parameter transferability within our study context. While {Van Rompaey, 2001 #10@@author-year} recognized technical limitations of WaTEM/ SEDEM in model transferability related to grid size and routing methods, our findings suggest additional challenges in accurately representing processes within micro-scale ~~conservation landscapes~~watersheds with specific in-field soil conservation practices (e.g. no-till farming). The need for watershed-specific calibration, even within relatively homogeneous landscapes with similar crop and soil properties, indicates that parameter calibration compensates for inherent model or

data limitations. At such fine scales, WaTEM/SEDEM may struggle to accurately represent the complex interactions between soil conservation practices~~measures~~ and erosion processes. However, it is important to note that these difficulties may stem from the low-magnitude nature of the erosion events observed in our study. As demonstrated in paired-plot experiments, natural variability is higher for small events {Wendt, 1986 #185}. Therefore, areas with higher erosion rates typically yield data that is less noisy and inherently easier for models to reproduce {Nearing, 1998 #134}.~~{Wendt, 1986 #185}{Nearing, 1998 #134}~~

Similar calibration challenges seem to exist more broadly in WaTEM/SEDEM applications across different landscape types and research questions, as evidenced by a wide range of calibrated k_{TC} values reported across different studies (Tab. 3), with $k_{TC/A}$ values varying from 10 to 174.4 m. As {Beven, 2006 #125@@author-year} argues, such calibration approaches may achieve mathematical fitting while concealing fundamental model inadequacies.

Structure-dominated watersheds

Unlike field-dominated watersheds, structure-dominated systems demonstrated different response patterns to extreme erosion events. In these watersheds, sediment generated during individual large erosion events (as observed in the field-dominated watersheds), is predominantly captured by grassed waterways and retention ponds {Fiener, 2003 #124;Fiener, 2005 #178}, thus reducing the variability of event sediment yields. This buffering effect explains why the model consistently overestimates sediment yield across all years for structure-dominated watersheds (Fig. 5~~4~~a-b), in contrast to the occasional underestimation observed in field-dominated systems (Fig. 4~~3~~a-d).

Only one exception to this pattern was observed: the model underestimated sediment yield in W05 during 1994, when the lower part of the grassed waterway required reseeding after losing its initial grass cover along the thalweg during a spring erosion event {Fiener, 2003 #124}. This exceptional case quantitatively demonstrates the role of functional grassed waterways, as the measured sediment yield in 1994 for W06 was substantially higher (0.78 t ha^{-1} yr^{-1}) than in subsequent years when the grassed waterway was fully established (averaging only 0.03 t ha^{-1} yr^{-1} from 1995-2001), representing an approximately 96 % reduction in sediment yield (Fig. 5~~4~~b).

The model's systematic overestimation of sediment yields in structure-dominated watersheds reveals limitations in representing the sediment trapping mechanisms of grassed waterways. The primary limitation is the model's inability to capture re-infiltration processes within the grassed waterway, which is not accounted for in WaTEM/SEDEM's transport capacity formulation. {Fiener, 2005 #178@@author-year} demonstrated that grassed waterway effectiveness depends strongly on morphological characteristics, particularly the cross-sectional shape, with flat-bottomed waterways showing substantially higher runoff reduction. The infiltration increases with length and flatter cross-sections of grassed waterways, which provide larger runoff widths and consequently greater infiltration areas. A previous study showed that in the upper part of the grassed waterway (W06), where WaTEM/SEDEM more substantially underestimates the sediment trapping, the long-term runoff and sediment yield reductions were respectively ~~was~~ about 90% and 97%, while it was about 10% and 77% in the lower part of the grassed waterway (W05) with a ditch-like cross-section (Fiener & Auerswald, 2003).

4.3 Spatial dynamics of erosion and deposition

The main reason for the reduction of sediment yield at the outlet within structure-dominated watersheds is visible in the eight-year mean map of behavioural model realisations (Fig. 8a). Depositional patterns are prominent along the flux pathway of the grassed waterway, particularly in W06. Because WaTEM/SEDEM is sensitive to the parameter controlling deposition inside these soil conservation structures ($k_{TC/G}$), the standard deviation in these areas is exceptionally high (Fig. 8b).

However, high uncertainty is not limited to the grassed waterways. It is also evident in depositional areas of field-dominated watersheds (most pronounced in W03). This suggests that deposition is generally prone to high uncertainties, regardless of the dominant structures. Furthermore, field-dominated watersheds exhibit high standard deviations within the fields themselves. This likely stems from parameter uncertainty regarding sediment supply, specifically the error surface parameter (e_{sur}, see Fig. 6b), which directly influences the sediment supply generated within the arable land.

4.4 Spatial aggregation

For the structure-dominated watersheds, spatial aggregation was critical for overcoming watershed-specific model failures. While the model failed to produce any behavioural realisations for W06 (even temporally lumped), the spatially aggregated group achieved 1.35% behavioural realisations. This aligns with the scale-dependency concepts reviewed by {de Vente, 2005 #44@@author-year}, who note that process dominance shifts with spatial scale, often allowing models to perform adequately at larger scales even if they miss finer processes.

For field-dominated watersheds, the spatial aggregation acted primarily as an averaging of varying crop states, smoothing out the heterogeneity of cover conditions, and any given watershed peculiarities. In contrast, for structure-dominated watersheds, spatial aggregation facilitates the identification of behavioural parameter spaces by masking local structural inadequacies, such as the deposition dynamics in grassed waterways. Consequently, the differences between spatially aggregated field-dominated and structure-dominated watersheds can be attributed to their structural components.

4.5~~3~~ Distribution of behavioural model parameter values

The *TC* within agricultural fields is primarily controlled by ~~a high~~ the transport coefficient $k_{TC/A}$ {Van Rompaey, 2001 #10}. Lower $k_{TC/A}$ values reduce TC, promoting in-field deposition and consequently decreasing sediment yield at the watershed outlet. Our analysis revealed behavioural model realisations across the full *a priori* selected range of $k_{TC/A}$ values, with no clear pattern for field-dominated watersheds, demonstrating no sensitivity even at very low $k_{TC/A}$ values near 1 or very high e_{sur} values of 0.5 (Fig. 6~~5~~a). This lack of sensitivity may be attributed to the retention ponds in W01 and W02 and the very low simulated erosion values. Since *TC* remained sufficiently high to transport the low sediment fluxes even with very low $k_{TC/A}$ values, sediment transport is thus supply-limited rather than constrained by transport capacity within the fields.~~This lack of sensitivity may be attributed to the implementation of retention ponds in W01 and W02 and by the very low simulated erosion values, as *TC* remained sufficiently high to transport the generally low sediment fluxes even with very low $k_{TC/A}$ values.~~

The low transport capacity coefficient for rougher surfaces, in case of this study for grassland $k_{TC/G}$, usually triggers deposition in these areas {Van Rompaey, 2001 #10}. Our analysis identified behavioural values for $k_{TC/G}$ between approximately 7.5 m to 15 m with a notable likelihood spike between approximately 9 m and 11 m, relatively low values compared to other studies (Tab. 3). While {Onnen, 2019 #139@@author-year} reported similarly low values for Danish landscapes, they explicitly attributed this to sandy soils in Denmark. However, our study area features predominantly silt loam and loamy soils, which are much more comparable to the Belgian soils (Tab. 3) where low k_{TC} values for rough surfaces were implemented {Peeters, 2008 #138;Verstraeten, 2002 #119;Van Rompaey, 2001 #10}.

Table 3: Comparison of k_{TC} parameter values of behavioural model realisations used in different studies with WaTEM/ SEDEM.

High k_{TC} values mostly used for arable land [m]	Low k_{TC} values mostly used for non-arable land [m]	Country	Source
150	not used	Germany	{Wilken, 2020 #141@@author-year}
10 to 24	1 to 12	Denmark	{Onnen, 2019 #139@@author-year}
100 & 150	25	Belgium	{Peeters, 2008 #138@@author-year}
75	42	Belgium	{Verstraeten, 2002 #119@@author-year}
75	42	Belgium	{Van Rompaey, 2001 #10@@author-year}
174.4	not used	Belgium	{Van Oost, 2000 #117@@author-year}

These low $k_{TC/G}$ values can have some possible interpretations: (i) most likely, the model is compensating for its inability to represent re-infiltration processes in grassed waterways, and/or (ii) the model may partly compensate for an overestimation of erosion rates in the draining fields. However, although the model outputs are fully spatially distributed (Fig. 8~~7a~~), it is not possible to compare the simulated patterns with spatially distributed observational data (e.g. aerial images, field surveys), because, except for some rare larger events, the effective soil conservation established prevents visible erosion features like rills.

In our study, WaTEM/SEDEM showed no sensitivity to parameters b_{dep} and p_{con} that represent the influence of linear landscape features. These parameters displayed homogenous likelihood distributions across the sampled parameter space (Fig. 7~~6~~b-c). This lack of sensitivity could stem from several factors: (i) sampling an overly narrow parameter space, (ii) limited influence of field borders in the studied watersheds due to the layout of the fields and watersheds with a small number of border situations, and/or (iii) a dominance of $k_{TC/G}$ implemented over a long grass structure, which may nullify the influence of b_{dep} and p_{con} in the model outputs, especially in watershed W05 and W06.

An additional limitation of the current parameterisation approach, particularly for grassed waterways, is its static nature. The effectiveness of grassed waterways and retention structures varies throughout the year due to seasonal vegetation changes {Fiener, 2003 #124}. Additionally, there is an important interaction between

sediment influx and trapping efficiency—as influx increases, the relative trapping efficiency typically decreases {Dermisis, 2010 #159;Fiener, 2018 #54}. {Dermisis, 2010 #159@@author-year} demonstrated this inverse relationship, showing that grassed waterway trapping efficiency decreases as peak runoff discharge increases, with notable breakpoints in efficiency between different flow rates. The current static connectivity and transport capacity parameters (p_{con}, b_{dep} and $k_{TC/G}$) cannot adequately capture these temporal variations and flux-dependent relationships, suggesting the need for a more dynamic parameterisation approach that accounts for both seasonal changes and influx response if the model is applied to an annual time-step.

5. Conclusion

We evaluated WaTEM/SEDEM's capability to simulate sediment yields in micro-scale watersheds ~~under~~ optimised for soil conservation and sediment transport reduction ~~practices~~ using a limits-of-acceptability approach within the GLUE framework. Our investigation examined model performance across different levels of spatiotemporal data aggregation and analysed the sensitivity of the model's response surface to the variability in the behavioural parameter space. Moreover, we used a two-step conditioning process, in which model parameters linked to in-field erosion processes were conditioned in field-dominated watersheds and later applied in structure-dominated watersheds, for which a separate set of connectivity parameters was also conditioned.

The model was unable to produce behavioural realisations for watersheds optimised for soil conservation and sediment transport reduction at annual time steps based on our strict limits of acceptability criterion despite the small absolute prediction errors over all model realisations (eight-year *MAE* = 0.1~~2~~42 t ha^{-1} yr^{-1} for field-dominated and eight-year *MAE* = 0.~~16~~29 t ha^{-1} yr^{-1} for structure-dominated watersheds). For the field-dominated watersheds, the model particularly struggled with simulating annual sediment yields. This is because soil conservation practices reduced the number of erosion events, yet some events (e.g., after potato harvest) retained a similar magnitude as in conventional cultivation. ~~For the field-dominated watersheds, the model particularly struggled with the simulation of annual sediment yields when individual extreme events dominated the annual sediment production.~~

Aggregating model outputs in time and space worked best for field-dominated systems, which compensated for the underestimation of soil conservation in controlling soil erosion and the model's inability to capture extreme events within an annual time step. ~~This finding confirms that~~While WaTEM/SEDEM is generally better suited for long-term erosion modelling, our findings confirm that this is especially the case for watersheds with optimised soil conservation and reduced sediment transport. ~~conservation planning than for making precise annual sediment yield predictions in areas with soil conservation practices.~~

The GLUE framework revealed specific patterns in the sampled parameter space, particularly the compensation mechanism between $k_{TC/A}$ and e_{sur} values for field-dominated watersheds, and the narrow behavioural parameter range of $k_{TC/G}$ values (7.5-15 m) for structure-dominated watersheds. Spatially, this sensitivity is mirrored by high standard deviations concentrated along the grassed waterways. In contrast, the standard deviation within arable

fields shows the influence of sediment supply parameterisation (e_{sur}) in field-dominated systems (Fig.8b). The likelihood distributions of $k_{TC/A}$ and especially e_{sur} enabled the pre-conditioning of structure-dominated watersheds, reducing parameter compensation effects that typically mask model structural deficiencies.

Ultimately, our study demonstrates that WaTEM/SEDEM can simulate the magnitude of very low sediment yields observed from soil conservation agricultural systems, provided that high spatiotemporal resolution input data and locally adapted USLE factors (e.g., the ABAG) ~~and locally adapted USLE factors (e.g., the ABAG for Southern Germany)~~ are available.~~are available.~~ However, capturing the combined effects of low in-field erosion and linear landscape features like grassed waterways, where concentrated runoff occurs, remains challenging for WaTEM/SEDEM, primarily due to the model's inability to represent re-infiltrating processes that are critical for sediment trapping in such structures. Additionally, our model evaluation approach revealed that model performance strongly depends on the spatiotemporal scale of analysis. While the model produced behavioural realisations for the aggregated eight-year monitoring period, it did not reliably simulate annual sediment yields. For long-term, large-scale soil conservation planning in which the effects of single erosive events on individual fields are less relevant for representing the system behaviour, WaTEM/SEDEM seems to be~~is~~ fit for purpose within our testing conditions.

Code availability

The R code used to compute individual factors and statistics is available at https://zenodo.org/records/18714865. The Python WaTEM/SEDEM code is available upon reasonable request.

~~The code is available on reasonable request.~~

Data availability

The input data are openly available and can be downloaded here: https://adgeo.copernicus.org/articles/48/31/2019/adgeo-48-31-2019.html (Last visited 11.07.2025). The specific data used to compute individual factors and statistics can be found at https://zenodo.org/records/18714865.

Author contribution

KDS: Conceptualisation, dData curation, fFormal analysis, iInvestigation, mMethodology, sSoftware, vVisualisation, wWriting (original draft preparation); PVGB: CConceptualisation, mMethodology, vValidation, wWriting (review and editing); HS: WWriting (review and editing); TS: SSupervision, wWriting (review and editing); PF: Conceptualisation, dData curation, pProject administration, sSupervision, vValidation, wWriting (review and editing).

Competing interests

Pedro V. G. Batista and Peter Fiener serve as Topic Editor and Executive Editor of SOIL, respectively.

Acknowledegments

We acknowledge the valuable dataset from the Forschungsverbund Agrarökosysteme München (FAM). The scientific activities of the FAM research network were financially supported by the German Federal Ministry of Education and Research (BMBF 0339370). We thank all researchers and technical staff involved in collecting and maintaining these long-term datasets, which made this study possible.

During the preparation of this work, the authors used Anthropic Claude 3.7 Sonnet to improve the readability and language of the manuscript. After using this tool, the authors reviewed and edited the content as needed and take full responsibility for the content of the published article.

Financial support

This research was funded by the German Research Foundation (DFG) through the DYLAMUST project (Project number: 509809226).

References